

Enhancement of local field by a two-dimensional array of dielectric spheres placed on a substrate

Masahiro Inoue

Institute of Applied Physics, University of Tsukuba, Sakura, Ibaraki 305 Japan

(Received 14 October 1986)

We consider a two-dimensional periodic array of dielectric spheres placed on a flat substrate and calculate its response to an incident electromagnetic wave. A remarkable feature of this system is the presence of electromagnetic resonance modes, which are shown to be closely related to the localized modes of a dielectric slab. When the resonance mode is excited, the local field near the sphere and consequently various electromagnetic quantities are enhanced. Enhancement factor of the Raman spectrum by adsorbed molecules is calculated and an optical bistability at a low laser power is predicted.

I. INTRODUCTION

Observation of surface-enhanced Raman scattering (SERS) (Ref. 1) has stimulated activity in surface electromagnetic (EM) theory.² By now it is widely accepted that excitation of surface plasmon polaritons (SPP's), which enhances the local-field intensity near the metal surface, is the main origin of SERS. The SPP mode has a dispersion relation outside the light cone and is not excited by the incident plane wave. When the momentum conservation parallel to the surface is violated by the surface roughness, however, the SPP mode is excited and the local field is enhanced. This SPP mechanism is confirmed by the observation of SERS from a smooth surface in attenuated total-reflection geometry,³ where evanescent waves from a prism can excite SPP modes. Furthermore, observation of enhanced second-harmonic generation⁴ verifies the enhancement of the local field on roughened metal surfaces.

A few years ago, we pointed out another mechanism of the local-field enhancement in terms of a two-dimensional array of dielectric spheres.⁵ Due to multiple scatterings between spheres, the spheres respond to the EM field collectively and the system is simulated by a thin dielectric slab with periodic modulation. The dielectric constant of the slab being larger than that outside, the slab works effectively as an attractive potential for the EM field and localized modes exist. Periodic modulation on the slab allows umklapp processes to occur, and these localized modes form energy bands in the Brillouin zone. Thus, some branches lie inside the light cone, which shows that they can be excited by the incident field. In this paper, we call them resonance modes. When excited, the resonance mode enhances the local-field intensity near the spheres and an anomaly appears in the reflectivity spectrum.⁶

A system of two-dimensional periodic array of spheres is rather artificial and is difficult to realize. In real systems, such as the crystalline phase of a monolayer of polystyrene particles floating on water⁷ or microstructures fabricated on a crystal surface,⁸ spheres are placed on a certain substrate which interacts with the resonance mode of spheres. Thus, the purpose of the present paper is to

clarify the character of the resonance mode for a more realistic system of arrayed spheres placed on a flat substrate.

When the substrate is made of a dielectric material of dielectric constant larger than that outside, the substrate is equivalent to an attractive potential for the EM field. Then we expect that the criterion for the presence of localized modes is more stringent and the envelope function of the localized mode extends toward the substrate. The latter effect reduces local-field intensities. Therefore, it is important to clarify the substrate effect. On the other hand, if the substrate is made of a metal, the interaction between the resonance modes and the SPP modes of the substrate is an interesting problem.

In the next section, basic formulas are given and expressions of local-field intensity, Raman enhancement factor, and energy flow of the EM field are derived. Numerical calculations are presented in Sec. III and the results are summarized in the last section. We point out that if we use the resonance modes, an optical bistability is realizable at a low laser power.

II. FORMULATION

The geometry of our system is shown in Fig. 1. We consider a square lattice structure in the x - y plane with lattice constant d . The radius of the sphere and its center to substrate-surface distance are denoted by a and Z_0 , respectively. The positive z direction is chosen from substrate to sphere. Therefore, for the incident wave vector, which has a negative z component, a superscript minus sign is added.

The integral equation for electric field of frequency ω is⁹

$$E(r) = E^0(r) + \sum_i \int \tilde{G}(r-r') v_i(r') E(r') dr',$$

$$v_i(r) = \frac{\omega^2}{c^2} [\epsilon_0 - \epsilon_i(r)] = (\kappa^2 - k_i^2) \theta(r), \quad (1)$$

$$\kappa = \frac{\omega}{c} (\epsilon_0)^{1/2} \text{ and } k_i = \frac{\omega}{c} (\epsilon_i)^{1/2},$$

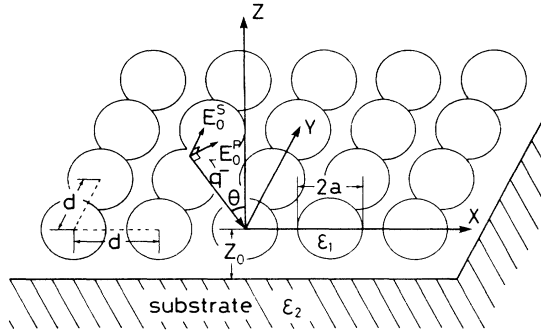


FIG. 1. Configuration of the system.

where ϵ_0 , ϵ_1 , and ϵ_2 are the dielectric constant of the vacuum, the sphere, and the substrate, respectively. $\Theta(r)$ is a step function equal to one inside the material and zero outside. For a material with a larger dielectric constant, the effective potential is more attractive. This ϵ dependence determines the essential features of the resonance mode. $\tilde{G}(r-r')$ is a tensor Green's function defined by

$$\tilde{G}_{i,j}(r-r') = \left[\delta_{i,j} + \frac{1}{\kappa^2} \nabla_i \nabla_j \right] G(r-r'), \quad (2)$$

$$G(r-r') = -\frac{1}{4\pi|r-r'|} e^{i\kappa|r-r'|}.$$

To solve Eq. (1), the most important step is to find a convenient expression for the tensor Green's function.

The difficulty of the present system comes from the fact that we need two kinds of basis functions, that is, vector spherical waves for a scattering by spheres and vector plane waves for a scattering by substrate. In a system with spherical symmetry, vector spherical waves¹⁰ are convenient basis functions, which are defined by

$${}^M E(f, \kappa, r, L) = \begin{pmatrix} 0 \\ \frac{1}{\sin\theta} \frac{\partial}{\partial\phi} \\ -\frac{\partial}{\partial\theta} \end{pmatrix} f(\kappa r) Y_L(\hat{r}),$$

$${}^N E(f, \kappa, r, L) = \begin{pmatrix} l(l+1) f(\kappa r) \\ [\kappa r f(\kappa r)]' \frac{\partial}{\partial\theta} \\ [\kappa r f(\kappa r)]' \frac{1}{\sin\theta} \frac{\partial}{\partial\phi} \end{pmatrix} \frac{1}{\kappa r} Y_L(\hat{r}), \quad (3)$$

where f is a spherical Bessel or a spherical Hankel function of the first kind and $L=(l,m)$ denotes both angular momentum and magnetic quantum number. A generalized spherical harmonic for a complex vector k is defined¹¹ for $m \geq 0$ by

$$Y_L(k) = Y_l^m(k)$$

$$= (-1)^m \left[\frac{2l+1}{4\pi} \frac{(l-m)!}{(l+m)!} \right]^{1/2} P_l^m \left[\frac{k_z}{k} \right] e^{im\phi},$$

$$Y_L^+(k) = Y_l^{m+}(k)$$

$$= (-1)^m \left[\frac{2l+1}{4\pi} \frac{(l-m)!}{(l+m)!} \right]^{1/2} P_l^m \left[\frac{k_z}{k} \right] e^{-im\phi}, \quad (4)$$

$$P_l^{-m} \left[\frac{k_z}{k} \right] = (-1)^m \frac{(l-m)!}{(l+m)!} P_l^m \left[\frac{k_z}{k} \right],$$

$$P_l^m(x) = (1-x^2) \frac{m}{2} \frac{d^m}{dx^m} P_l(x).$$

The tensor Green's function is then given¹² by

$$\tilde{G}_{\alpha,\alpha'}(r-r') = \frac{1}{\kappa^2} \delta(r-r') \delta_{\alpha,r} \delta_{\alpha',r}$$

$$- i\kappa^\beta E_\alpha(f, \kappa, r, L) \frac{1}{l(l+1)} \beta E_{\alpha'}^+(g, \kappa, r', L), \quad (5)$$

where $f_l(\kappa r) = j_l(\kappa r)$, $g_l(\kappa r') = h_l(\kappa r')$ for $r < r'$, and $f_l(\kappa r) = h_l(\kappa r)$, $g_l(\kappa r') = j_l(\kappa r')$ for $r > r'$. Here and hereafter, the summation over $\beta=(M,N)$ and $L=(l,m)$ is understood. Due to the periodic structure of the array, the electric field takes the following form inside the n th sphere:

$$E(r) = \beta E(j, k_1 r_n, L) \alpha_L^\beta(i) e^{iq^- R_n}, \quad (6)$$

where we put $r = r_n + R_n$ and $k_1 = \omega \sqrt{\epsilon_1}/c$ is the wave vector inside the sphere. $\alpha(i)$, an expansion coefficient of the electric field inside the sphere, is independent of R_n and the site dependence is described by the phase factor $\exp(iq^- R_n)$. By expanding an incident vector plane wave by a linear combination of vector spherical waves of wave vector κ ,

$$E^0(r) = \beta E(j, \kappa, r, L) \alpha_L^\beta(0),$$

Eq. (1) gives

$$v_l^\beta \alpha_L^\beta(i) = (t^{-1} - \Gamma)^{-1} \alpha(0), \quad (7)$$

where

$$v_l^M = ix [x j_l'(x) j_l(z) - z j_l(x) j_l'(z)],$$

$$v_l^N = ix \left[z j_l(z) \frac{1}{x} [x j_l(x)]' - x j_l(x) \frac{1}{z} [z j_l(z)]' \right],$$

$$u_l^M = ix [z h_l(x) j_l'(z) - x h_l'(x) j_l(z)],$$

$$u_l^N = ix \left[x h_l(x) \frac{1}{z} [z j_l(z)]' - \frac{1}{x} [x h_l(x)]' z j_l(z) \right],$$

$$x = \kappa a, \quad z = k_1 a,$$

$$t_l^\beta = \frac{v_l^\beta}{u_l^\beta},$$

and

$$\Gamma_{L,L'}^{\beta,\beta'} = \sum_{n \neq 0} \Delta_{L,L'}^{\beta,\beta'}(h, R_n) e^{iq \cdot R_n}.$$

From the vector-translational theorem,¹³ we obtain

$$\begin{aligned} \Delta_{L,L'}^{M,M}(h, R) &= \frac{1}{2l(l+1)} [l(l+1) + l'(l'+1) - l''(l''+1)] C(L | L' L'') h_{l''}(\kappa R) Y_{L''}^+(R), \\ \Delta_{L,L'}^{M,N}(h, R) &= -i \frac{1}{2l(l+1)} \left[\frac{2j+1}{2j-1} \right]^{1/2} h_j(\kappa R) Y_j^+(R) \\ &\quad \times [2m' \sqrt{(j-m_3)(j+m_3)} C(L | L', j-1, m_3) \\ &\quad + \sqrt{(j-m_3)(j-m_3-1)(l'+m')(l'-m'+1)} C(L | l', m'-1, j-1, m+1-m') \\ &\quad - \sqrt{(j+m_3)(j+m_3-1)(l'-m')(l'+m'+1)} C(L | l', m'+1, j-1, m-1+m')], \end{aligned}$$

$$\begin{aligned} m_3 &= m - m', \\ \Delta^{NN} &= \Delta^{MM}, \quad \Delta^{NM} = \Delta^{MN}, \end{aligned}$$

where

$$\begin{aligned} C(l_1 m_1 | l_2 m_2, l_3 m_3) \\ = 4\pi i^{l_1 - l_2 - l_3} \int Y_{l_1}^+(q) Y_{l_2}(q) Y_{l_3}(q) d\Omega. \end{aligned}$$

We used the Ewald's method¹⁴ to evaluate the structure factor Γ , which describes multiple scatterings between spheres.

On the other hand, in a system with a flat surface, vector plane waves are convenient. The transmitted and reflected waves of a semi-infinite substrate are given by

$$E(r) = E(k) e^{ik \cdot r} \quad \text{for } z < -Z_0,$$

where

$$\begin{aligned} E_i(k) &= T_{ij}(q) E_j^0, \\ T_{ij}(q) &= \frac{2\gamma}{\gamma + \gamma'} \delta_{i,j} - \frac{2\gamma q_i^- (\gamma - \gamma')}{(\gamma + \gamma')(\kappa^2 + \gamma\gamma' - \gamma^2)} \delta_{j,z}, \end{aligned}$$

and

$$E(r) = E^0(r) + E^R(r) \quad \text{for } z > -Z_0,$$

$$\begin{aligned} \tilde{G}_{i,j}(r-r') &= \frac{-1}{(2\pi)^3} \int \frac{1}{q^2 - \kappa^2} \left[\delta_{i,j} - \frac{1}{\kappa^2} q_i q_j \right] e^{iq \cdot (r-r')} dq \\ &= \frac{1}{\kappa^2} \delta(r-r') \delta_{i,z} \delta_{j,z} - \frac{i\pi}{(2\pi)^3} \int \frac{1}{\gamma} \left[\delta_{i,j} - \frac{1}{\kappa^2} q_i^\pm q_j^\pm \right] e^{iq^\pm \cdot (r-r')} dq_{\parallel}, \end{aligned} \quad (9)$$

where

$$q^\pm = (q_{\parallel}, \pm\gamma), \quad z \gtrless z'$$

which is an integral over the wave-vector component parallel to the surface. When the magnitude $|q_{\parallel}|$ is larger than κ ($=\omega\sqrt{\epsilon_0}/c$), the z component of the wave

where

$$E_i^R(r) = R_{i,j}(q) E_j^0 e^{iq \cdot r}, \quad (8)$$

$$\begin{aligned} R_{i,j}(q) &= \left[\frac{\gamma - \gamma'}{\gamma + \gamma'} \delta_{i,j} - \frac{2\gamma}{\kappa^2 + \gamma\gamma' - \gamma^2} \frac{\gamma - \gamma'}{\gamma + \gamma'} q_i^+ \delta_{j,z} \right. \\ &\quad \left. + \frac{2\gamma(\gamma - \gamma')^2}{(\gamma + \gamma')(\kappa^2 + \gamma\gamma' - \gamma^2)} \delta_{i,z} \delta_{j,z} \right] e^{2i\gamma Z_0}, \\ \gamma &= (\kappa^2 - q_{\parallel}^2)^{1/2} \end{aligned}$$

and

$$\gamma' = \left[k_{\perp}^2 - k_{\parallel}^2 \right]^{1/2} = \left[\frac{\omega^2}{c^2} \epsilon_2 - k_{\parallel}^2 \right]^{1/2}$$

are the z component of the wave vector outside and inside the substrate, respectively, and $k_{\parallel} = q_{\parallel}$ is the wave-vector component parallel to the surface. The origin of the coordinate is taken at the center of a sphere and the factor $\exp(2i\gamma Z_0)$ gives an additional phase change of the reflected wave which propagates a distance $2Z_0$ between the sphere and the substrate. To derive these, we used the transversality of the electric field and the following expression of the tensor Green's function

vector is pure imaginary and the Green's function represents a propagation of evanescent waves.

In our geometry of spheres on a substrate, there occurs a multiple scattering between a sphere and the substrate. To describe this process, we must rewrite the vector spherical wave emitted from a sphere as a linear combina-

tion of vector plane waves. This is performed by introducing a new vector $\xi(q)$, which is a function of wave vector and angular momentum, and is defined by

$$\xi_L^M(q) = A_l \begin{pmatrix} 0 \\ \frac{-m}{\sin\theta} Y_L(q) \\ -i \frac{\partial}{\partial\theta} Y_L(q) \end{pmatrix}, \quad \xi_L^N(q) = A_l \begin{pmatrix} 0 \\ -\frac{\partial}{\partial\theta} Y_L(q) \\ -i \frac{m}{\sin\theta} Y_L(q) \end{pmatrix},$$

and

$$\xi_L^M(q)|_z = A_l m Y_L(q),$$

$$\xi_L^N(q)|_z = A_l (\sin\theta) \frac{\partial}{\partial\theta} Y_L(q),$$

where

$$A_l = \frac{4\pi i^{-l-1}}{l(l+1)}. \quad (10)$$

In terms of these vectors, the Green's function is written as

$$\begin{aligned} \tilde{G}_{i,j}(r-r') &= -\frac{i\pi}{(2\pi)^3} \int \frac{1}{\gamma} \left[\delta_{i,j} + \frac{1}{\kappa^2} \nabla_i \nabla_j \right] e^{iq^\pm(r-r')} dq_{\parallel}, \\ &= -\frac{i\pi}{(2\pi)^3} \int \frac{1}{\gamma} e^{iq^\pm r} \xi_L^\beta(q^\pm) \beta E^+(j, \kappa, r', L) dq_{\parallel}, \\ &= -\frac{i\pi}{(2\pi)^3} \int \frac{1}{\gamma} \beta E(j, \kappa, r, L) \xi_L^{\beta+}(q^\pm) e^{-iq^\pm r'} dq_{\parallel} \end{aligned} \quad (11)$$

for $z \geq z'$

which represents a conversion of the vector spherical wave into a sum of vector plane waves of both propagating and evanescent, and vice versa. Finally, by taking into account multiple scatterings both between spheres, and spheres and the substrate, we obtain for $z > a$.

$$E(r) = E^0(r) + E e^{iq^+ r} + \sum_G F(G) e^{iq_G^+ r},$$

where

$$E = R(q) E^0,$$

$$F(G) = \frac{1}{2\kappa s} \frac{1}{\gamma_G} [\xi(q_G^+) + R(q_G) \xi(q_G^-)] l(l+1) \tilde{\alpha},$$

$$\tilde{\alpha} = v \alpha(i) = (t^{-1} - \Gamma - \tilde{\Gamma})^{-1} \alpha(2), \quad (12)$$

$$\alpha(2) = \alpha(0) + \xi^+(q^+) R(q) E^0,$$

$$\tilde{\Gamma} = \sum_G \xi^+(q_G^+) R(q_G) \frac{1}{2\kappa s} \frac{1}{\gamma_G} \xi(q_G^-) l(l+1).$$

Here, $\tilde{\Gamma}$ describes a multiple scattering between a sphere and the substrate. The diffracted waves are proportional to the sum of the incident wave and the reflected wave from the substrate. The electric field inside the sphere is given by Eq. (6) with $\alpha(i)$ replaced by the present expres-

sion. Due to the periodic structure of the spheres, the reflected wave is given by a linear combination of diffracted waves, both propagating and evanescent, whose wave-vector components parallel to the surface are shifted by the reciprocal-lattice vectors. When the determinant of the matrix $(t^{-1} - \Gamma - \tilde{\Gamma})$ approaches zero, the electric field around the sphere is enhanced and an anomaly appears in the reflectivity spectrum. This is the mathematical description of the resonance mode. We have used the following relations

$$\sum_n e^{i(k-q)R_n} = N \sum_G \delta(q - k - G),$$

$$\sum_{q_{\parallel}} = \frac{Ns}{(2\pi)^2} \int dq_{\parallel},$$

where N and s are the number of the spheres and the unit cell area, respectively.

The electric field intensity averaged inside the sphere and its normal component averaged slightly outside the sphere are given by

$$\begin{aligned} I &= \frac{1}{v} \int^a |E(r)|^2 dr \\ &= \frac{1}{v} \int |\beta E_L(j, k, r, L)|^2 |\alpha_L^\beta(i)|^2 dr \\ &= \frac{3}{4\pi} \sum f_l^\beta |\alpha_L^\beta(i)|^2, \end{aligned}$$

where

$$\begin{aligned} f_l^M &= \frac{1}{2} l(l+1) [j_l^2(z) - j_{l-1}(z) j_{l+1}(z)], \\ f_l^N &= l(l+1) \frac{1}{z^2} j_l(z) (z j_l(z))' + f_l^M, \end{aligned} \quad (13)$$

for real k , and

$$\begin{aligned} f_l^M &= l(l+1) [z^* j_l(z) j_l'(z^*) - z j_l'(z) j_l(z^*)] / (z^2 - z^{*2}), \\ f_l^N &= \frac{l(l+1)}{|z|^2} j_l(z) [j_l(z^*) + z^* j_l'(z^*)] + \frac{z^*}{z} f_l^M, \end{aligned}$$

for complex k

$$\begin{aligned} I_r &= \frac{1}{4\pi} \int |E_r(a+0)|^2 d\Omega \\ &= \frac{1}{4\pi} \int \left| \frac{\epsilon_1}{\epsilon_0} \right|^2 |E_r(a-0)|^2 d\Omega \\ &= \frac{1}{4\pi} \left| \frac{z}{x} \right|^4 \int |{}^N E(j, k_1, a, L)|^2 |\alpha_L^N(i)|^2 d\Omega \\ &= \frac{1}{4\pi} \left| \frac{z}{x} \right|^4 \left| \frac{l(l+1)}{z} j_l(z) \alpha_L^N(i) \right|^2. \end{aligned}$$

The continuity of the normal component of the displacement field ϵE is used for the latter expression. Both M and N fields contribute to the average intensity, while only N field contributes to the normal component.

The flow of the EM energy is described by the Poynting's vector. The total energy absorbed inside the metal substrate is given by integrating its z component over the x - y plane above the substrate. The result is

$$\begin{aligned}
E(r) &= E^0 e^{iq^-r} + E e^{iq^+r} + \sum_G F(G) e^{iq_G^+r}, \\
- \int P_z dr_{\parallel} &= \frac{-c}{8\pi} \operatorname{Re} \int (E_x H_y^* - E_y H_x^*) dr_{\parallel} \\
&= \frac{-c^2}{8\pi\omega} \left[(-|E^0|^2 + |E|^2) \gamma_0 + \sum_{G<} |F(G)|^2 \gamma_G + 2 \operatorname{Re} E^* \frac{1}{2\kappa s} [\xi(q^+) + R(q)\xi(q^-)] l(l+1)\tilde{\alpha} \right]. \quad (14)
\end{aligned}$$

The first two terms give the energy flow of the incident wave and the reflected wave from the substrate. The third term gives the energy of the diffracted waves. The sum over the reciprocal-lattice vectors is restricted such that the diffracted waves have real wave vectors. The last term is a cross term of the reflected waves.

Lastly, we consider that some molecules are adsorbed on the spheres uniformly and calculate an enhancement factor F of the Raman scattering intensity. The Raman tensor of the molecule is assumed to be diagonal and have nonzero element only in the direction normal to the sphere surface. Raman shift is neglected and the scattered light is calculated in the direction of the specular reflection. After some calculation, we obtain

$$\begin{aligned}
F &= \frac{3}{2} \frac{1}{(4\pi)^3} \left| \frac{z}{x} \right|^4 \left[\frac{j_l(z)}{z} \right]^* \left[\frac{j_{l'}(z)}{z} \right] l(l+1)l'(l'+1) \alpha_L^N(i) [\alpha_{L'}^N(i)]^* i^{l_2-l'_2-1+l'} C(l_2, m_2 | l', m_2, l'', 0) \\
&\quad \times C(l, m | l', m, l'', 0) \hat{\Gamma}_{L_2, L'_2}, \\
\hat{\Gamma}_{L_1, L'_1} &= \eta_{L, L_1}^{\beta*} \tilde{\xi}_{L'}^{\beta+}(q^+) \tilde{\xi}_{L'}^{\beta-}(q^+) \eta_{L', L'_1}^{\beta}, \\
\eta_{L, L'}^{\beta} &= [(t^{-1} - \Gamma - \tilde{\Gamma})^{-1}]_{L, L'}^{\beta, N} \left[(t_i^N)^{-1} + \frac{h_{l'}(x)}{j_{l'}(x)} \right] \frac{j_{l'}(x)}{x}, \\
\tilde{\xi}_{L'}^{\beta}(q^+) &= [\xi_{L'}^{\beta}(q^+) + R \xi_{L'}^{\beta}(q^-)] l(l+1). \quad (15)
\end{aligned}$$

The factor $\alpha_L^N(i)$ comes from the local field at the adsorbed molecules and the factor $\eta_{L, L'}^{\beta}$, gives the second-stage enhancement, i.e., enhancement of the dipole radiation of the molecule by the excitation of the resonance modes.

III. NUMERICAL RESULTS

First we neglect the substrate and show various features of the resonance modes.

Figure 2 shows integrated density of states (IDS) (Ref. 14) for the EM field, specular reflectivity, electric field intensity averaged inside the sphere, its normal component averaged slightly outside the sphere, and the Raman enhancement factor. The average intensities are scaled by the incident field intensity I_0 . Solid curves are for p polarization and dotted curves are for s polarization. The incident wave vector lies in the x - z plane and the incidence angle is 20° . The dielectric constant of the sphere and its radius are chosen as $\epsilon_1=3$ and $a/d=0.4$, respectively. The frequency of the electric field is scaled as $Z=d/\lambda (=d\omega\sqrt{\epsilon_0}/2\pi c)$; the lattice constant divided by the wavelength in vacuum. A sharp increase in IDS means that there exists a sharp resonance level at that frequency. We call it a resonance mode. An important fact is, when the resonance mode is excited, the local-field intensity is enhanced and its peak value approaches to almost 10^2 . It is to be noticed that, a large enhancement of the electric field is not necessarily associated with a large signal in the specular reflectivity. In fact, the dominant peak in I_r/I_0 at $Z=0.87$ gives only a small dip and a

hump to the spectrum. In these cases, anomaly appears in the intensity of diffracted waves. The singularity at $Z=0.74$ comes from the first multichannel threshold,⁶ and diffraction occurs at higher frequencies. Below this frequency, a complete reflection is realized when the resonance mode is excited. This comes from the fact that

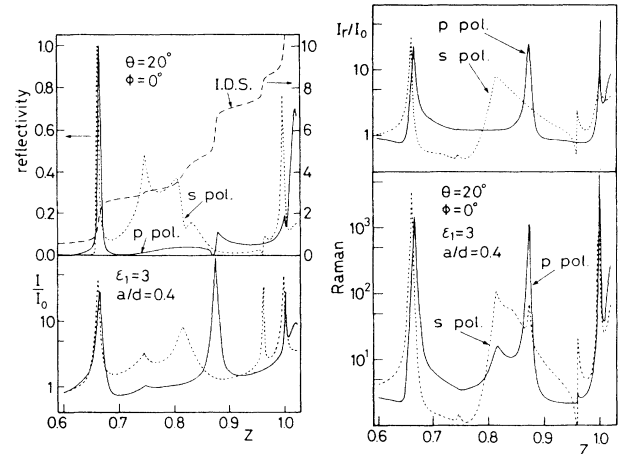


FIG. 2. Integrated density of states, specular reflectivity, electric field intensity averaged inside the sphere, its normal component averaged slightly outside the sphere, and enhancement factor of the Raman intensity emitted by molecules adsorbed on the sphere. Solid curves are for p polarization and dotted curves are for s polarization. The abscissa is a scaled frequency defined by $Z=d/\lambda$. The incidence angle is 20° and the dielectric constant of the sphere is chosen as $\epsilon_1=3$. $a/d=0.4$.

there exists only one mode in both the transmitted and the reflected waves which are connected to the localized mode of the spheres. The anomaly of the normal component is characterized by the polarization of the incident field and appears at the same frequency as the anomaly of the averaged intensity. This point is different from the case of a single sphere; only the N field determines the former while the M field dominantly contributes to the latter and their resonance frequencies are different in general. The Raman intensity reflects the enhancement factor of the normal component. However, in the second stage, the dipole field emitted by the molecule has both s and p characters and so, the Raman spectrum is peaked at both resonance frequencies. The peak value of the Raman spectrum is of the order of 10^4 , which is comparable to that realized by roughened metal surfaces.

Next, the dielectric constant dependence of the resonance mode is shown in Fig. 3. A larger dielectric constant is equivalent to a deeper attractive potential for the EM field. Therefore, with the increase of the dielectric constant, the resonance modes shift to the low-frequency side monotonically. On the other hand, the change of the spectral shape is not simple; some modes narrow and the associated intensities increase but other modes broaden and their intensities decrease. This point is also different

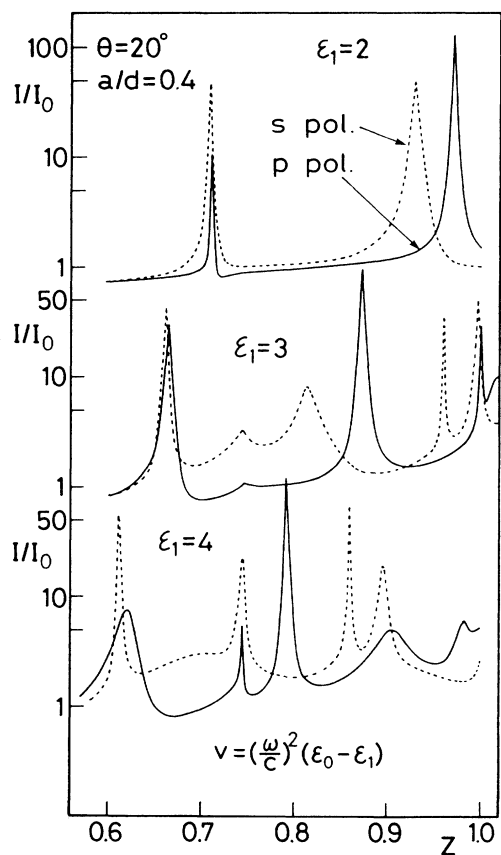


FIG. 3. Dielectric constant dependence of local-field intensity spectrum.

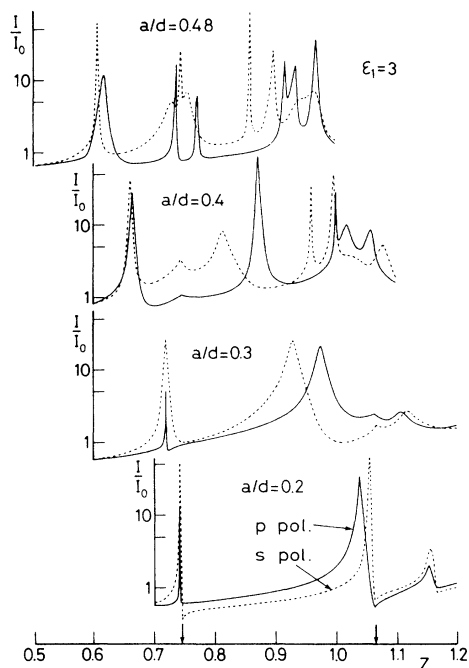


FIG. 4. Radius dependence of the resonance modes. The lattice constant is fixed.

from the case of a single dielectric sphere, where spectrum sharpens and intensity increases with the dielectric constant. The radius dependence is shown in Fig. 4. The lattice constant is fixed and $\epsilon_1=3$. At low densities (the cases of small radius as shown at the bottom of the figure), the frequency of the resonance mode is close to that

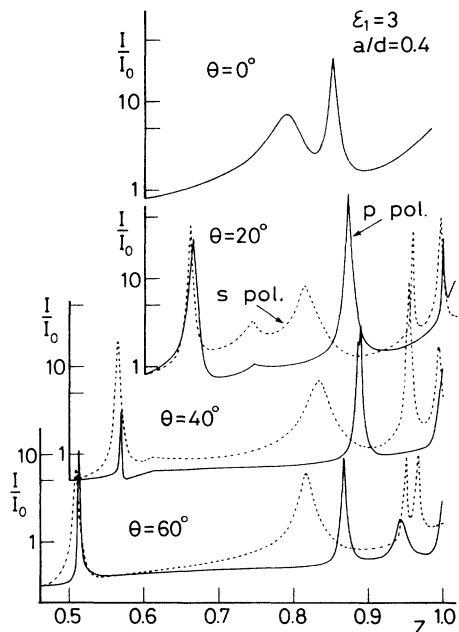


FIG. 5. The incidence angle dependence of the resonance modes. $\epsilon_1=3$ and $a/d=0.4$.

of a free photon and singularities appear near multichannel thresholds which are shown by arrows in the figure. With the increase of the radius, an attractive potential region increases and the resonance-mode frequencies decrease. When a/d is increased from 0.3 to 0.4 (0.4 to 0.48), the number of the resonance modes increases abruptly at $Z = 1.06$ ($Z = 0.74$) for the both polarizations. That is, new resonance modes appear at multichannel thresholds. Lastly, the incidence angle dependence is shown in Fig. 5. The frequency of the lowest resonance mode shifts about $\Delta Z = -0.3$ when the incidence angle is increased from zero to $\theta = 60^\circ$. The behaviors of high-frequency modes are complicated. Although resonance frequencies depend on these parameters, the intensity enhancement factor is of the order of 10^2 except at large incidence angles or at low density of spheres.

The resonance mode is closely related to a localized mode of a thin dielectric slab with the same dielectric constant. With increase of the dielectric constant or thickness of the slab, the localized modes make low-frequency shifts and an excited state starts its dispersion curve on the line $\omega = ck_{\parallel}$. Figure 6 shows an empty lattice band structure of the localized mode of a slab, whose thickness L is chosen such that its volume is equal to that of the arrayed spheres with $a/d = 0.4$. The abscissa gives the parallel component of the wave vector in units of

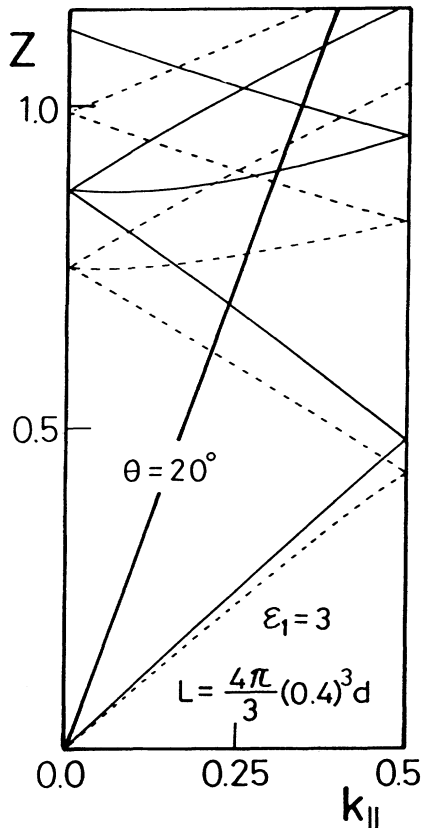


FIG. 6. The empty lattice band structure of the localized mode of a thin dielectric slab.

$2\pi/d$. The solid bold line shows the dispersion relation of the incident wave with $\theta = 20^\circ$. The crossing of these two curves indicates that the localized modes are excited by umklapp processes due to the periodic structure. The frequency and the number of the resonance modes are approximately reproduced by this model. Furthermore, the following features of the resonance modes are reproduced, (1) with increase of the dielectric constant or the radius of the sphere, resonance modes make low-frequency shifts, (2) with the incidence angle, the lowest resonance mode shifts to the low-frequency side, while high-frequency modes form complicated band structures, (3) a new resonance mode appears at multichannel thresholds. Thus, the nature of the resonance modes of a two-dimensional array of spheres is close to that of the localized modes of a dielectric slab with appropriate thickness and is quite different from that of a single sphere. This comes from the collective response of the spheres brought about by the multiple scattering of EM waves between spheres.

Next, substrate effects are investigated. Figure 7 shows the average intensity inside the sphere as a function of the substrate dielectric constant ϵ_2 and the distance Z_0 . The dielectric constant of the sphere is fixed at $\epsilon_1 = 4$ and $a/d = 0.4$. For the curve at the top of the figure, substrate is not present. With increase of ϵ_2 , the resonance modes are broadened and the peak intensity is reduced by

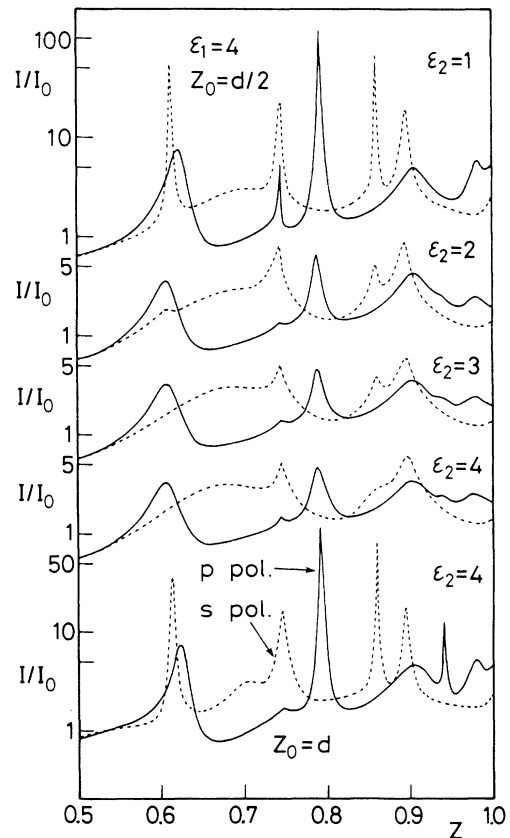


FIG. 7. The resonance modes of the arrayed dielectric spheres placed on a dielectric substrate of ϵ_2 .

an order of magnitude at $Z_0=d/2$. The effective potential of the dielectric substrate becomes more attractive with ϵ_2 and the envelope function of the resonance mode extends toward the substrate. This effect reduces the local-field intensity, though the resonance frequencies decrease only a little. As shown at the bottom of the figure, the curve for $Z_0=d$ is almost the same with the curve without substrate as shown at the top. An exception is a sharp peak for *p* polarization near $Z=0.94$. This peak originates from an excitation of a resonance mode by a diffracted wave which is reflected back to the array by the substrate. From these results, we can say that the envelope functions of the resonance modes are confined within the thickness of $z=d$. This fact is consistent with the slab model. The parallel component of the incident wave vector is $Z \sin(\theta)$ in the unit of the reciprocal-lattice

vector $K=2\pi/d$. The *z* component of the wave vectors of the evanescent waves are then given by $\gamma=\{Z^2-[Z \sin(\theta)-n]^2-m^2\}^{1/2}$ with integer *m* and *n*, because the parallel components are shifted by reciprocal-lattice vectors. For $m=0$ and $n=1$ or $m=1$ and $n=0$, the magnitude of γ is about 0.6 for $Z=0.6$, which gives $\exp(-|\gamma|Z_0K)=0.15$ for $Z_0=d/2$ and 0.022 for $Z_0=d$, i.e., overlap is appreciable in the former, but is negligible in the latter. Therefore, the dielectric substrate gives an important modification to the resonance mode when Z_0 is less than the lattice constant.

The situation is quite different for a metal substrate. In addition to the resonance mode of dielectric spheres, there exists SPP mode localized on the metal surface and their interaction is expected to modify their characters. Figures 8 and 9 show the effects of the silver substrate for $d=0.5 \mu\text{m}$, $a/d=0.4$, $\epsilon_1=3$ and $\theta=20^\circ$. For the present parameters, $Z=1$ corresponds to $\hbar\omega=2.45 \text{ eV}$, which is well below the surface plasmon energy of silver and a flat substrate shows an almost complete reflection at the frequencies investigated. $Z_0=d$ in Fig. 8 and $Z_0=d/2$ in Fig. 9. In addition to the intensity enhancement factor, we show the energy absorbed in the substrate, which comes mainly

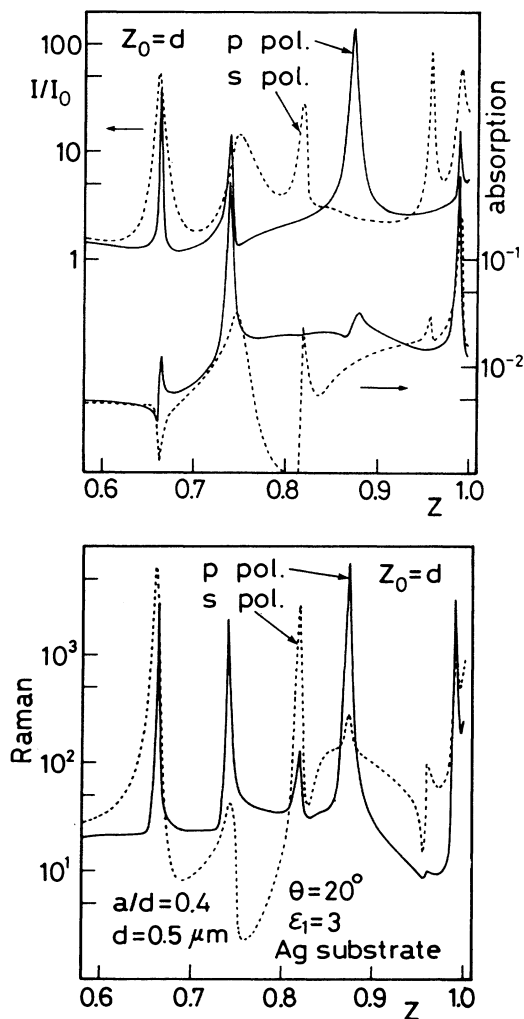


FIG. 8. Average intensity inside the sphere, EM energy absorbed in the metal substrate and enhancement factor of the Raman intensity observed from the direction of specular reflection. Silver is assumed as the substrate. $\theta=20^\circ$, $a/d=0.4$, $d=0.5 \mu\text{m}$, and $Z_0=d$.

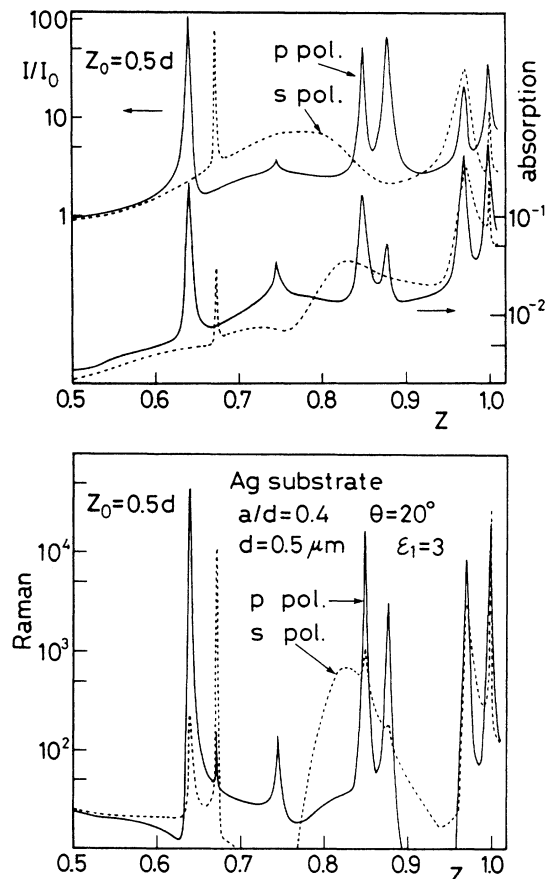


FIG. 9. The same as in Fig. 8 except that $Z_0=d/2$.

from the excitation of SPP modes in the substrate. Reflectivity is given by subtracting absorption from unity. When $Z_0 = d$, the coupling of the two modes is expected to be small. In fact, the enhancement spectrum is almost the same as that obtained in the case without substrate and the sharp peaks in the absorption spectrum at $Z = 0.73$ and $Z = 1$ are interpreted as resonant excitation of SPP mode. Figure 10 shows the dispersion relations of the SPP mode and evanescent waves from the arrayed spheres. The abscissa gives the parallel component of the wave vector in units of $2\pi/d$. Corresponding reciprocal-lattice vectors are inserted. The crossing of these curves occurs at exactly the same frequencies as the absorption peaks. That is, SPP modes are excited by evanescent waves emitted from the periodic array through the umklapp processes.

On the other hand, when Z_0 is reduced to $d/2$, the coupling of the two modes modifies their characters and a low-frequency shift at $Z = 0.64$ and splittings around $Z = 0.86$ and $Z = 0.98$ are observed. Further enhancement of the local-field intensity and the Raman scattering efficiency are realized. As the SPP mode is p polarized, interaction is strong for p polarization. These features of the resonance-mode frequencies are again reproduced by a localized mode of a dielectric slab placed on the metal substrate. In Fig. 11, the dispersion relation is shown for p polarization. A dielectric slab of thickness L is placed on a silver substrate with spacing D . The imaginary part of the dielectric constant is neglected for the metal substrate. The bold curves correspond to the present parameter. At low frequencies, the two dispersion relations, the dispersion relations of the SPP mode and the localized mode of the slab, are close to each other. Due to their

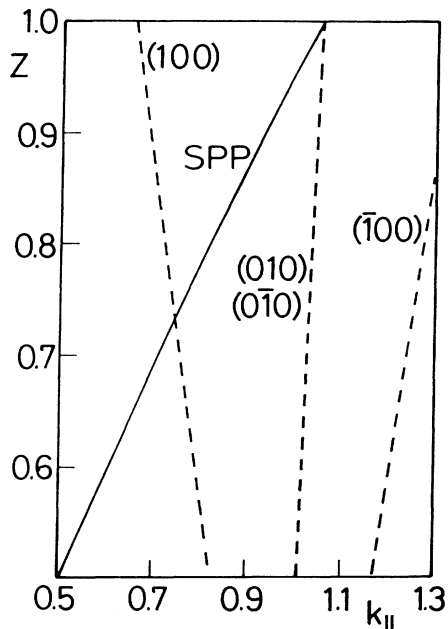


FIG. 10. The dispersion relations of SPP mode and evanescent waves emitted by the periodic array of spheres.

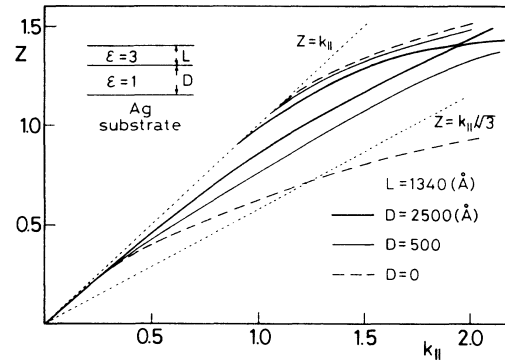


FIG. 11. The dispersion relation of the localized mode in a thin dielectric slab, which interacts with the SPP mode of the metal substrate.

repulsive interaction, one of the modes is pushed up beyond the line $Z = k_{\parallel}$ and disappears and the other mode is pushed down. This strong coupling at low frequencies comes from the fact that the envelope function of the SPP mode extends deep into the vacuum and overlaps largely with the localized mode of the slab: The damping constant of the SPP mode is given by $\gamma = \sqrt{(\epsilon_2 + 1)/\epsilon_2} \kappa$, which approaches $\kappa = 2\pi/\lambda$ at low frequencies ($\epsilon_2 \rightarrow -\infty$). At high frequencies, there exists a SPP-like mode. The low-frequency shift of the low-lying modes and their splittings at high frequencies are thus explained.

The character of the localized mode depends on the distance D . At $D = 2500$ Å, the two modes preserve their original characters of the SPP mode and the localized mode of the slab except at low frequencies. When the two dispersion curves approach to each other, anticrossing occurs at around $k_{\parallel} = 1.8$ and $Z = 1.4$. Decreasing the distance, dispersion relation of the lower branch is pushed down below the line $Z = k_{\parallel}/\sqrt{\epsilon_1}$ at $k_{\parallel} > 1.25$ as shown by a dashed curve for $D = 0$; the dielectric slab is in contact with the substrate. As the dispersion relation of the localized mode of the slab lies above this line, this fact shows that the lower branch is SPP-like which exists near the boundary between the metal substrate and the dielectric slab. At low frequencies, however, the envelope of the SPP mode extends far into the vacuum penetrating through the dielectric slab. Then the effect of the dielectric slab becomes negligible and the dispersion relation approaches the line $Z = k_{\parallel}$ instead of $Z = k_{\parallel}/\sqrt{\epsilon_1}$. High-frequency mode is localized mainly in the dielectric slab.

IV. SUMMARY AND DISCUSSIONS

In this paper, various features of the resonance modes are clarified for a two-dimensional array of dielectric spheres placed on a flat substrate. When excited, the resonance modes enhance local-field intensities by 2 orders of magnitude. With increase of the radius or the dielectric constant of the sphere the resonance mode shifts to the low-frequency side. The lowest resonance frequency decreases monotonically with incidence angle, while, high-frequency modes show complicated band structures.

These features are closely related to those of the localized mode of a dielectric slab. If the substrate is a dielectric, envelope of the resonance mode extends toward the substrate and the peak intensity is reduced by an order of magnitude at $Z_0=d/2$. That is, the substrate effect is crucial at short distance. When the substrate is made of a metal, the interaction between the resonance mode and the SPP mode changes their characters and frequency shifts or splittings occur at short distances. In this case, local-field intensity is enhanced further by excitation of the SPP mode.

Lastly, we show that we can use these features of the resonance modes to realize optical bistability at a low laser power.¹⁶ Assume that the dielectric constant of the sphere has a third-order nonlinearity as

$$\epsilon_1(I) = \epsilon_1 + 4\pi\chi^3 I,$$

where we put $\chi^3 = 10^{-5}$ esu. Then we fix the laser frequency at slightly below the resonance frequency. A schematic diagram of optical bistability is given in Fig. 12. First consider the intensity enhancement factor I/I_0 as a function of the dielectric constant. Increasing ϵ_1 , the resonance-mode frequency decreases (see Fig. 3) and I/I_0 at a fixed frequency ω first increases, attains its peak value of the order of 10^2 , and then decreases. On the other hand, the dielectric constant increases linearly with the internal intensity I . Therefore, in a certain region of I_0 , the two curves have three crossing points. This indicates optical bistability. As an illustration, we consider the case shown in Fig. 9. We use the enhanced local field by the lowest p -mode and fix the frequency at $Z=0.635$. Stable states as a function of incident intensity are calculated numerically by iteration. Bold solid curves in Fig. 13 show specular reflectivity versus incident laser power and thin solid curves show their corresponding nonlinear dielectric constant. With increase of the laser power, the high-reflectivity branch jumps to the low-reflectivity branch and with decrease of the power, it jumps back to the original branch. Even when ϵ_1 has an imaginary part, as curve B shows, optical bistability is realizable. Here, the optical

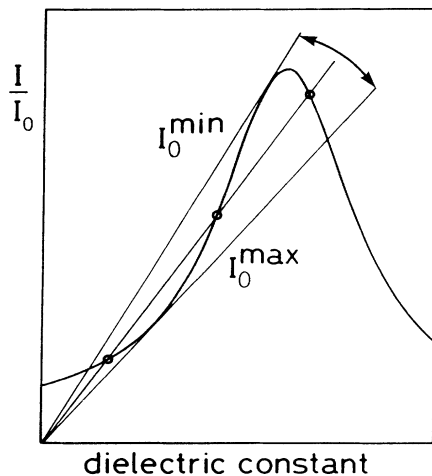


FIG. 12. A schematic diagram illustrating optical bistability.

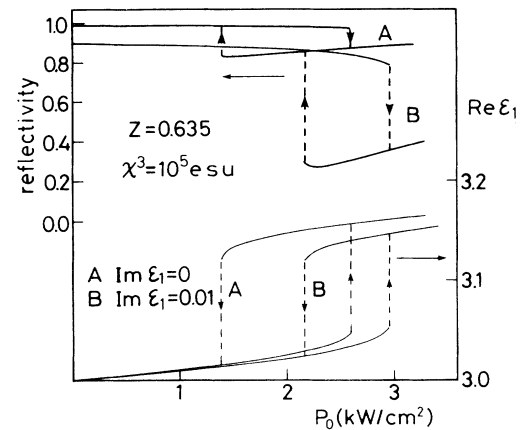


FIG. 13. An optical bistability realized by the resonance mode. Reduction of the laser power comes from the local-field enhancement.

bistability at a low laser power is realized both by large enhancement of the local-field intensity and the sensitiveness of the resonance-mode frequency to the dielectric constant.

We have replaced local-field intensities by the average intensity in the nonlinear Maxwell equation. Figure 14 shows position-dependent intensity inside the sphere. Except the fourth direction, perpendicular to both the incident electric vector and the incident wave vector, uniformity is quite good. Thus, our approximation of replacing the local-field intensities by the average intensity is shown to be rather good. Furthermore, as the resonance-mode frequency is a macroscopic quantity determined by the collective nature of the spheres, inhomogeneity of the local field is expected to be unimportant.

We have shown that the local-field enhancement realized by the excitation of the resonance mode can be used to observe enhanced Raman scattering from adsorbed molecules, and a possibility of optical bistability is predicted. Furthermore, the Raman scattering from inside the sphere is expected to be enhanced. This phenomenon is useful for the investigation of surface

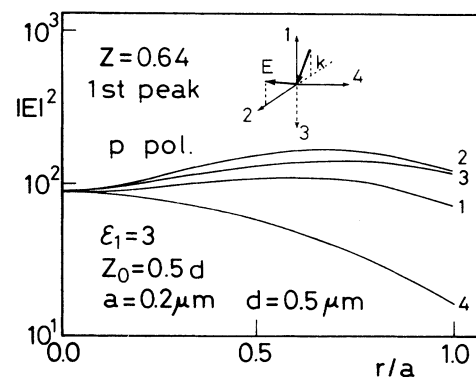


FIG. 14. Position dependence of the electric field intensity inside the sphere for the p polarized lowest resonance mode.

modes of fine particles. As the excitation of SPP-like mode is possible, second-harmonic generation at a metal substrate is also expected.

The merit of this system is that the resonance-mode frequency can be controlled easily by (1) the lattice constant (the resonance-mode frequency is scaled as $Z=d/\lambda$), (2) the radius of the sphere, and (3) the incidence angle. This point is useful for the experiments. We used a specific model of an arrayed dielectric sphere. However, as we have shown, essential features of the resonance modes are

reproduced by localized modes of a thin dielectric slab. This suggests the generality of the features obtained. That is, arrayed spherical particles or even a grating of a dielectric material coated on a metal substrate is also expected to have similar features. Thus, we can conclude that the local-field enhancement by the resonance-mode mechanism is a general phenomena in microstructures fabricated on crystal surfaces and hope that it will find various applications in surface nonlinear optics.

-
- ¹I. Pockrand, *Surface Enhanced Raman Vibrational Studies at Solid/Gas Interface*, Vol. 104 of *Springer Tracts in Modern Physics* (Springer, Berlin, 1984); R. K. Chang and B. L. Laube, *CRC Crit. Rev. Solid State Mater. Sci.* **12**, 1 (1984); A. Otto, in *Light Scattering in Solids IV*, edited by M. Cardona and G. Guntherodt (Springer, Berlin 1984).
- ²A. Wokaun, in *Solid State Physics*, edited by H. Ehrenreich, D. Turnbull, and F. Seitz (Academic, New York, 1938) Vol 38; M. Moskovits, *Rev. Mod. Phys.* **57**, 783 (1985); G. W. Ford and W. H. Weber, *Phys. Rep. C* **113**, 195 (1984).
- ³Y. J. Chen, W. P. Chen, and E. Burstein, *Phys. Rev. Lett.* **361**, 1207 (1976); S. Ushioda and Y. Sasaki, *Phys. Rev. B* **27**, 1401 (1983).
- ⁴C. Y. Chen, A. Y. B. de Castro, and Y. R. Shen, *Phys. Rev. Lett.* **46**, 145 (1981); A. Wokaun, J. G. Bergman, J. D. Heritage, A. M. Glass, P. F. Liao, and D. H. Olson, *Phys. Rev. B* **24**, 849 (1981).
- ⁵M. Inoue and K. Ohtaka, *Phys. Rev. B* **26**, 3487 (1982), *J. Phys. Soc. Jpn.* **52**, 1457 (1983).
- ⁶K. Ohtaka and M. Inoue, *Solid State Commun.* **40**, 425 (1981); M. Inoue and K. Ohtaka, *Phys. Rev.* **25**, 689 (1982).
- ⁷P. Pieransky, *Phys. Rev. Lett.* **45**, 569 (1980).
- ⁸P. F. Liao, J. G. Bergman, D. S. Chemla, A. Wokaun, J. Melngails, A. M. Hawryluk, and N. P. Economou, *Chem. Phys. Lett.* **82**, 355 (1981).
- ⁹K. Ohtaka, *J. Phys. C* **13**, 667 (1980).
- ¹⁰J. A. Stratton, *Electromagnetic Theory* (McGraw-Hill, New York, 1941).
- ¹¹S. Y. Tong, *Prog. Surf. Sci.* **7**, 1 (1975).
- ¹²M. Inoue and K. Ohtaka, *J. Phys. Soc. Jpn.* **52**, 3853 (1983). A complex vector function with a superscript plus sign is defined by a Hermite conjugate of the function, except for spherical Bessel or Hankel functions and spherical harmonics. The former are unchanged and the latter are replaced by Y^+ defined in Eq. (4).
- ¹³O. R. Cruzan, *Quart. Appl. Math.* **20**, 33 (1962).
- ¹⁴K. Kambe, *Z. Naturforsch* **A22**, 322 (1967).
- ¹⁵K. Ohtaka and M. Inoue, *Phys. Rev. B* **25**, 677 (1982).
- ¹⁶M. Inoue *Phys. Rev. Lett.* **58**, 871 (1987).